Experimental Cell Research 167 (1986) 16–28

Reorganization of α-Actinin and Vinculin in Living Cells Following ATP Depletion and Replenishment

YU-LI WANG*

Department of Molecular and Cellular Biology, National Jewish Center for Immunology and Respiratory Medicine, Denver, CO 80206, and Department of Biochemistry, Biophysics, and Genetics, University of Colorado Health Sciences Center, Denver, CO 80220, USA

Although it is known that the depletion of cellular ATP induces a dramatic, reversible disruption of microfilament structures, the morphological pathway remains obscure. I have studied this process by following directly the dynamic redistribution of fluorescently labeled α-actinin and vinculin which had been microinjected into living mouse 3T3 fibroblasts. Before treatment, microinjected α-actinin displayed characteristic distribution along stress fibers, whereas vinculin was localized predominantly at adhesion plaques. The first response after adding NaN_3 and 2-deoxyglucose was the retraction of lamellipodia, followed, over a period of 2 h, by a dramatic contraction of stress fibers and loosening of focal contacts. Vinculin plaques shrank from an elongated shape to small aggregates. During recovery, which was initiated by removing NaN_3 and 2-deoxyglucose from the medium, lamellipodia appeared rapidly and α-actinin dispersed from contracted aggregates. Some partially dispersed aggregates later served as initiation sites for the formation of stress fibers. The recovery of vinculin plaques occurred predominantly through direct elongation, and focal contacts developed concomitantly. A small fraction of vinculin aggregates, however, moved into the perinuclear region without developing into adhesion plaques, and some new vinculin plaques formed de novo. Possible mechanisms involved and relationships to disruptions induced by other agents are discussed.

The static aspects of the organization of actin filaments in cultured cells have been investigated extensively during recent years. For example, many cultured non-muscle cells contain a well-organized set of actin filament bundles, termed stress fibers. At least one end of a stress fiber is associated with the plasma membrane, opposite to the site of an adhesion plaque (also referred to as focal contact) on the external surface (for a review see [1]). Besides actin filaments, a number of accessory proteins such as myosin, tropomyosin, and α-actinin have been identified along stress fibers. In addition, several proteins, including vinculin and talin, are concentrated at adhesion plaques [2–4].

It is well known that the organization of stress fibers can change reversibly in response to various treatments such as trypsinization [5], neoplastic transformation [1, 6] and depletion of cellular ATP [7, 8]. However, since most observations

* To whom offprint requests should be sent. Address: Department of Molecular and Cellular Biology, National Jewish Center for Immunology and Respiratory Medicine, 1400 Jackson Street, Denver, CO 80206, USA.

0014-4827/86 $03.00

were made using static techniques such as immunofluorescence and electron microscopy, little is known about either the exact pathways of disruption and recovery, or the relationship between stress fibers, adhesion plaques, and amorphous aggregates commonly observed in disrupted cells.

A particularly attractive model system for studying such questions is the disruption induced by the depletion of cellular ATP. In both cultured fibroblasts and epithelial cells, stress fibers disappear soon after the treatment and are replaced by numerous actin-containing aggregates in the cytoplasm [7, 8]. The cell, however, remains spread after the treatment, thus facilitating detailed light microscopic observations. In addition, since the disruption is rapidly reversible upon the removal of the agents, the recovery process can also be studied.

In this study, fluorescent analogue cytochemistry [9, 10] was employed to examine the disruption and recovery of α-actinin- and vinculin-containing structures following the depletion and replenishment of cellular ATP. Since the experiments were performed with fluorescently labeled functional proteins microinjected into living cells, dynamic changes in specific components could be studied directly. The results provide clear evidence regarding the fate of stress fibers and adhesion plaques following the treatment, the mechanism of the formation of aggregates, and the pathway of the reassembly of stress fibers and adhesion plaques during recovery.

MATERIALS AND METHODS

Preparation of Fluorescent Analogues

Alpha-actinin was isolated from chicken gizzards and labeled with iodoacetamidotetramethylrhodamine (IATR) as described previously [11]. The conjugate had a dye/protein molar ratio of 1.2 to 1.8. Smooth muscle vinculin was isolated from chicken gizzards according to Evans et al. [12]. Vinculin was labeled with tetramethylrhodamine isothiocyanate (TRITC, 10% on celite, Research Organics, Cleveland, Ohio) by adding the dye to vinculin solution in 100 mM potassium borate, pH 9.0, to reach an initial dye/protein molar ratio of 20. After stirring at 4°C for 2 h, the celite particles were removed by centrifugation. Lysine was then added to the solution to a concentration of 50 mM. The solution was further incubated at 4°C for 2 h, followed by chromatography in an SM-2 (Bio-Rad Laboratories, Richmond, Calif. [11]) column. The fractions containing the conjugate were pooled, dialysed extensively against 1 mM PIPES, 0.1 mM dithiothreitol, pH 6.95, and concentrated to obtain a vinculin concentration of 5 mg/ml. The dye/protein molar ratio was estimated to be 3.0.

All conjugates were stored for up to a month on ice and were clarified at 100 000 g for 20 min before microinjection. The purity of the proteins and the removal of unbound dye were determined by SDS gel electrophoresis. The ability of the α-actinin conjugate to cross-link actin filaments was determined by falling-ball viscometry [13]. Labeled α-actinin retained 100% of the cross-linking activity of the unlabeled protein.

Cell Culture, Microinjection, and Microscopy

Mouse 3T3 fibroblasts (Swiss albino or BALB/c) were obtained from the American Type Culture Collection (Rockville, Md.) and were cultured in Dulbecco's modified Eagle medium (KC Biologicals, Lenexa, Kans.) supplemented with 10% calf serum (Colorado Serum, Denver, Colo.), 50 U/ml penicillin, and 50 μg/ml streptomycin. Cells were plated onto microinjection dishes [14] 12 h before an experiment in Eagle's minimum essential medium (MEM) (KC Biologicals), supplemented with 10% calf serum and antibiotics. Microinjection was performed as described previously [14]. The volume

injected was estimated to be 2–5% of the cell volume. Following microinjection, cells were incubated for at least 2 h to allow incorporation of injected analogues into cellular structures.

During observation, cells were maintained on a Zeiss IM-35 inverted microscope in humid air supplemented with CO_2 at a temperature of 31–32°C [14]. Fluorescence images were observed with a 100×/N.A. 1.30 neofluar objective, a 63×/N.A. 1.25 neofluar phase objective or a 40×/N.A. 1.0 apochromatic objective, using epi-illumination with a 100 W quartz–halogen lamp operated at 6 V or less. To avoid cross-over of rhodamine fluorescence into the fluorescein image during comparison of the two fluorophores, an additional barrier filter (cut-off wavelength 550 nm) was added to the fluorescein filter set. Interference reflection microscopy (IRM) was performed with an epi-illuminator, a fluorescein filter set without the barrier filter, and an aperture inserted near the dichromatic mirror.

Depletion of cellular ATP was induced by replacing the medium in microinjection dishes with the same medium containing 20 mM NaN_3 and 10 mM 2-deoxyglucose (Sigma Chemicals, St. Louis, Mo.). Staining with fluorescein phalloidin (Molecular Probes, Eugene, Ore.) was performed as described by Amato et al. [15].

Image Recording and Processing

Images were detected using a Dage-MTI (Michigan City, Ind.) ISIT image intensifier coupled to an image processing system. During an experiment, raw images were fed from the image intensifier into the image processing system, which averaged 128 successive frames and stored the averaged image on a hard disk. Image averaging dramatically improved the resolution and the signal-to-noise ratio. Stored images were later retrieved and an image of the dark-current was subtracted from each image to remove background. Images were then photographed from a video monitor on Tri-X film and developed in Diafine.

RESULTS AND DISCUSSION

Redistribution of α-Actinin and Vinculin Following Depletion of Cellular ATP

3T3 mouse fibroblasts were microinjected with either IATR-labeled α-actinin or TRITC-labeled vinculin. After 2 h of incubation, injected α-actinin became associated with stress fibers and adhesion plaques, whereas vinculin was enriched primarily at adhesion plaques [2, 3, 16, 17]. No discrete structure was detected with fluorescently labeled ovalbumin in either untreated or ATP-depleted cells (not shown).

Following depletion of cellular ATP, the earliest response detected with IATR α-actinin was the retraction of lamellipodia (fig. 1*a*, *b*, arrows). This was followed, over a period of 2 h, by a dramatic disruption of stress fibers (fig. 2). All fibers showed a decrease in length, with a concomitant increase in intensity. Frequently, the fiber changed from a straight morphology into a curved or twisted shape (fig. 2, long arrows). At high magnifications, a decrease in the length of 'minisarcomeres' along stress fibers was observed (fig. 3). These observations indicate that stress fibers underwent contractions which, as shown in fig. 2, occurred predominantly toward the distal ends where adhesion plaques were located.

The contraction of stress fibers appears to be contradictory to the report that MgATP is required [18]. However, NaN_3 and 2-deoxyglucose may induce contractions through rapid disruptions of cytoplasmic free (Ca^{2+}) and/or pH before the total depletion of cytoplasmic ATP. In addition, some MgATP may be stably associated with stress fibers and thus not directly affected by the treatment.

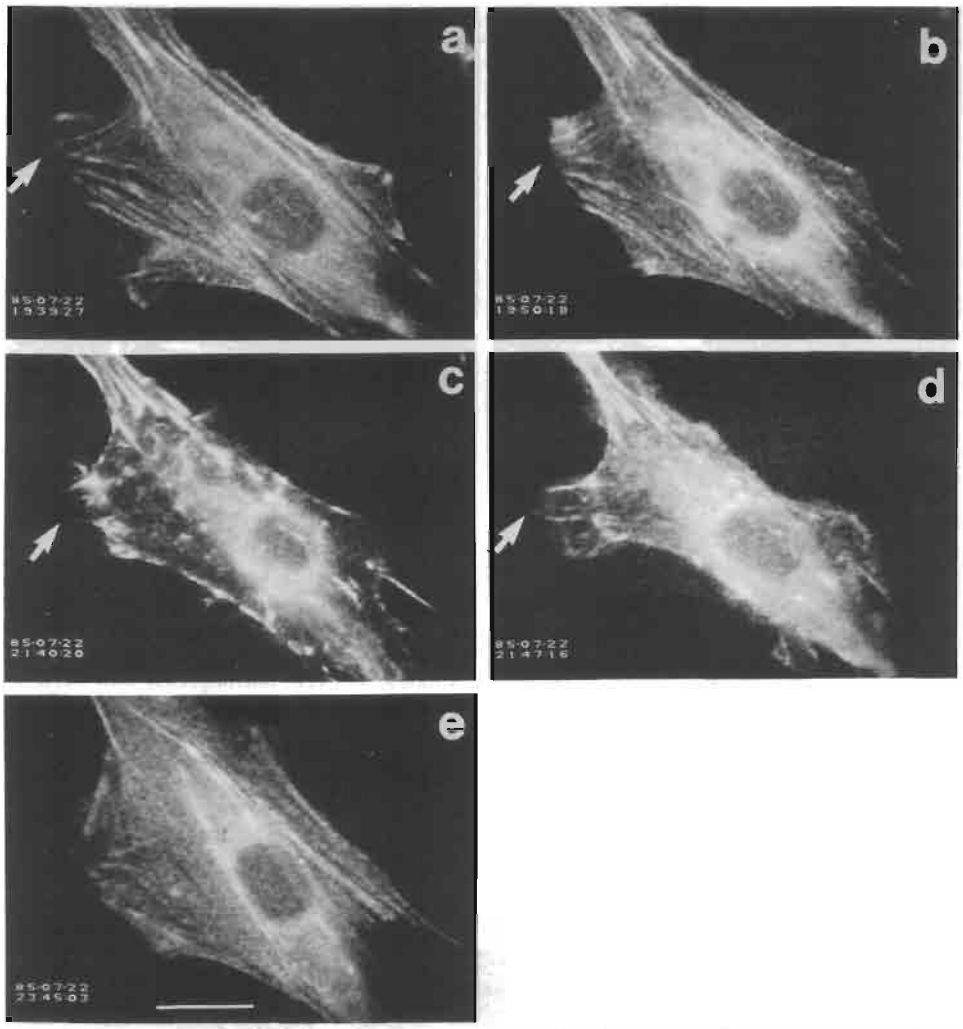

Fig. 1. Effect of ATP depletion on lamellipodia. A mouse 3T3 cell, microinjected with IATR α-actinin, was treated with NaN_3 and 2-deoxyglucose at 19:41. The agents were later removed at 21:44. The time of image recording is indicated at the lower left corner of each micrograph. A lamellipodium was visible 2 min before treatment (*a*, *arrow*), but retracted 9 min after treatment (*b*, *arrow*). The cell contained no stress fibers but numerous bright aggregates and relatively low diffuse fluorescence 2 h after treatment (*c*). As soon as 3 min after the removal of the agents (*d*), a lamellipodium (*arrow*) reappeared at the same location as in (*a*). The cell resumed a normal morphology 2 h after removing the agents (*e*). Bar, 20 μm.

Besides contraction, many long fibers fragmented (fig. 2, short arrows). It is clear that contraction and fragmentation were not induced simply by illumination or by medium replacement, since removal of NaN_3 and 2-deoxyglucose initiated a rapid recovery to a morphology similar to that of untreated, unilluminated cells

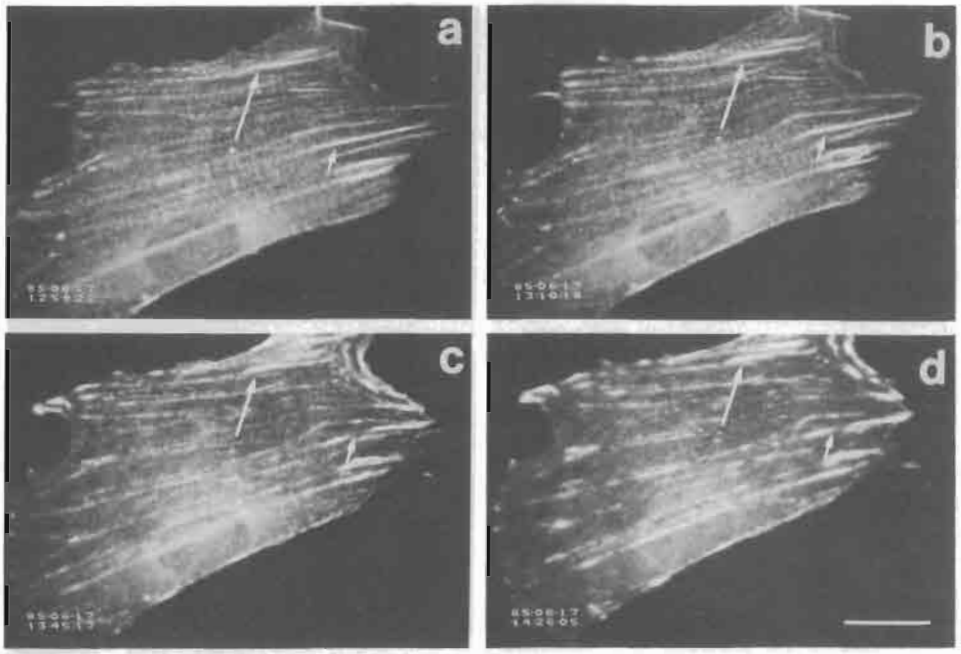

Fig. 2. Effects of ATP depletion on stress fibers. A mouse 3T3 cell, microinjected with IATR α-actinin, was treated with NaN_3 and 2-deoxyglucose at 13:00. The time of image recording is indicated at the lower left corner of each micrograph. Fluorescence images were recorded at (*a*) 1 min before treatment; (*b*) 10 min; (*c*) 45 min and (*d*) 86 min after treatment. Before treatment, an extensive array of stress fibers was present in the cytoplasm. After treatment, stress fibers showed an increase in fluorescence intensity and changed from straight bundles into curved or twisted structures (*long arrows*). Some fibers fragmented (*short arrows*). The recovery of this cell is shown in fig. 5. Bar, 20 μm.

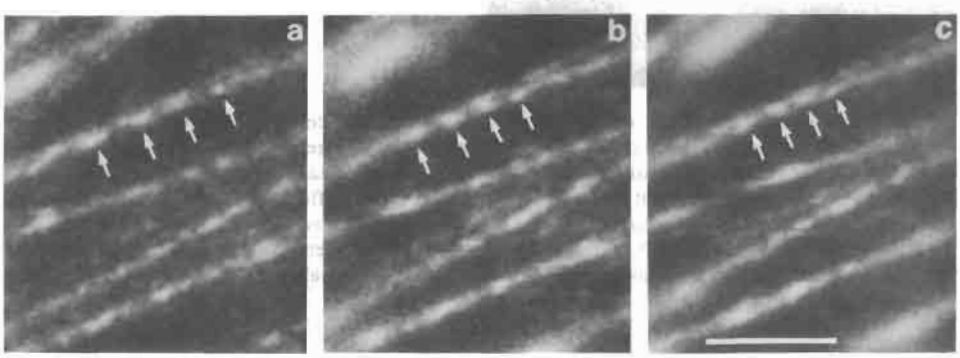

Fig. 3. High magnification micrographs of stress fibers undergoing contraction following ATP depletion. The cell was injected with IATR α-actinin, which clearly defined the minisarcomeres along stress fibers (*arrows*). Shortening of the minisarcomeres was apparent from micrographs taken before (*a*), 39 min (*b*) and 77 min (*c*) after the addition of NaN_3 and 2-deoxyglucose. Bar, 5 μm.

(described later). The distribution of actin in treated cells, as revealed by staining injected cells with fluorescein–phalloidin, was very similar to that of α-actinin (not shown) and to that reported previously [7, 8].

Focal contacts, as revealed by IRM (fig. 4, arrows), rapidly lost their darkness following the depletion of ATP, indicating that the association between the membrane and the underlying substrate was loosened. Vinculin plaques, however, remained detectable and stationary. They lost their normal elongated shape and shrank into small aggregates without an apparent increase in intensity (fig. 4, arrows).

The molecular mechanisms involved in the shrinkage of vinculin plaques and the loosening of focal contacts are not clear at present. It has been suggested that the elongated morphology of vinculin plaques is a result of stretching by associated actin filaments [6]. When stress fibers collapse toward the adhesion plaques, elongated vinculin plaques may then shrink into small aggregates. It has also been shown that the presence of adhesion plaques in isolated membranes are sensitive to changes in pH [19]. The effects of ATP depletion can similarly be mediated through changes in cytoplasmic pH or other environmental parameters.

Distribution of α-Actinin and Vinculin during Recovery from ATP Depletion

The first detectable response following the removal of NaN_3 and 2-deoxyglucose was the formation of lamellipodia (fig. 1*d*, arrow), which were highly active during the first 10 min of recovery but subsided later. The cell apparently can 'remember' the location of lamellipodia prior to ATP depletion, since new lamellipodia were always detected near their locations before the treatment (fig. 1*a*, *d*, arrows). Aggregates of α-actinin did not simply stretch back into fibrous structures. Instead, they underwent a rapid decrease in intensity during the first 20 min of recovery (figs 5, 6, arrows). This suggests a dissociation of molecules, possibly actin–myosin rigor complexes, following the availability of ATP.

Although many aggregates dispersed completely (fig. 6*a–c*, short arrows), some partially dispersed aggregates can serve as initiation sites for the assembly of new stress fibers, which subsequently elongated unidirectionally toward the nucleus (fig. 6*a–e*, long arrows). The assembly of stress fibers appeared very similar to those observed in unperturbed cells and in cells recovering from explantation [14, 20]. During elongation, some aggregates moved toward the nucleus (fig. 5, arrowheads), as if they were pushed centripetally by elongating fibers. Within 2 h after the removal of the agents, injected α-actinin resumed a pattern of distribution similar to that in untreated cells, although the exact location of stress fibers could be very different from that before treatment (figs 1*a*, *e*, 2*a*, 5*d*). Staining of α-actinin injected cells with fluorescein–phalloidin during recovery revealed a distribution of F-actin similar to that of α-actinin, except for a more discontinuous appearance of α-actinin along the fiber (fig. 7). This suggests that a similar pathway may be followed by actin.

Three different events were detected with vinculin aggregates during recovery.

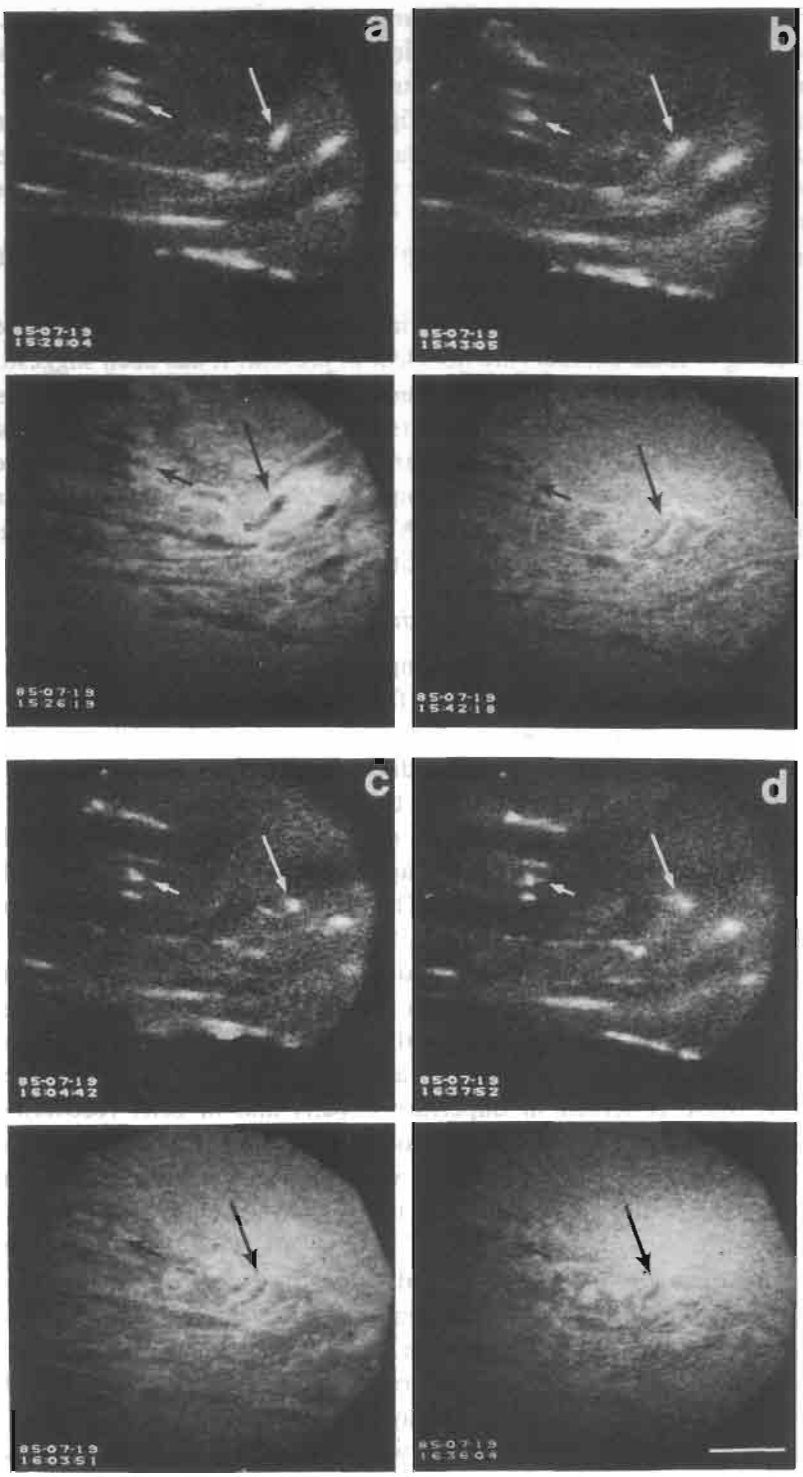
a
85-07-19
15:28:04
b
85-07-19
15:43:05
85-07-19
15:26:18
85-07-19
15:42:18
c
85-07-19
16:04:42
d
85-07-19
16:37:52
85-07-19
16:03:51
85-07-19
16:36:04

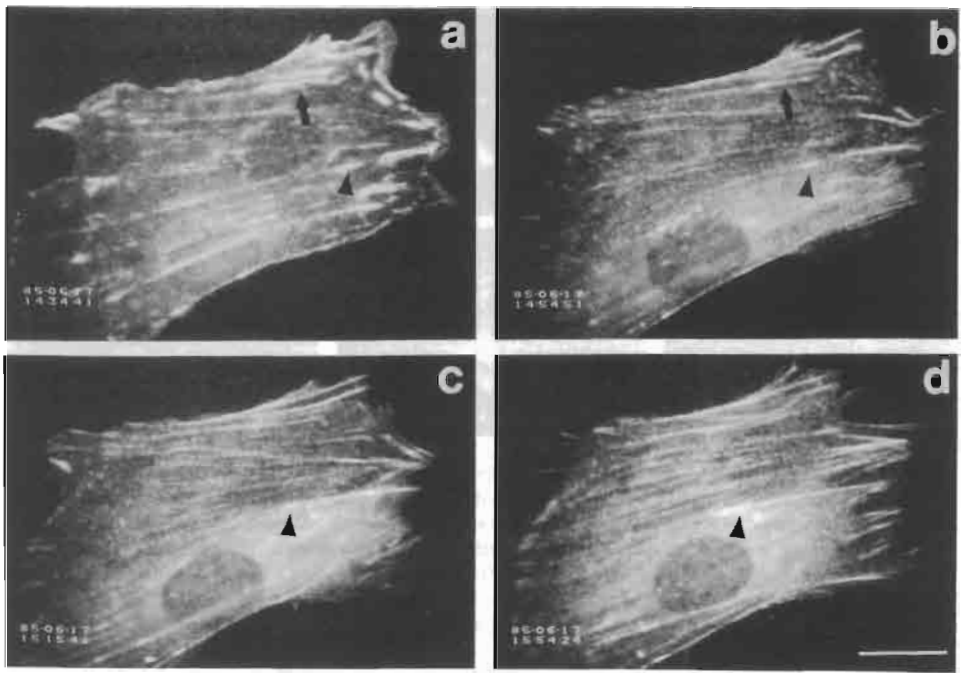

Fig. 5. Reorganization of α-actinin during recovery from ATP depletion. The disruption of this cell was shown previously in fig. 2. NaN_3 and 2-deoxyglucose were washed off at 14:33. The time of recording is indicated at the lower left corner of each micrograph. Fluorescence images were recorded at 1 min (*a*), 21 min (*b*), 42 min (*c*), and 81 min (*d*) after removal of the agents. The bright aggregates underwent a rapid decrease in fluorescence intensity (*arrows*). Some aggregates moved toward the nucleus as if they were pushed by elongating stress fibers (*arrowheads*). Bar, 20 μm.

Most aggregates appeared to elongate directly into plaques typical of untreated cells (fig. 8, arrows). Unlike α-actinin aggregates, the recovery occurred without an apparent initial decrease in fluorescence intensity. A small fraction of aggregates, however, moved into the perinuclear region without recovering into adhesion plaques (fig. 9, arrowheads). In addition to direct recovery and movement, formation of new vinculin plaques was also detected (fig. 9 *b–d*, arrows).

Fig. 4. Effects of ATP depletion on vinculin distribution and adhesion plaques. A mouse 3T3 cell, previously microinjected with TRITC vinculin, was treated with NaN_3 and 2-deoxyglucose at 15:30. The time of image recording is indicated at the lower left corner of each micrograph. Fluorescence images (*upper panels*) and IRM images (*lower panels*) were recorded at (*a*) approx. 3 min before treatment; (*b*) 13 min; (*c*) 34 min and (*d*) 67 min after treatment. Before treatment, adhesion plaques appeared as dark elongated patches in the IRM image (*a, lower panel*), and corresponded to elongated patches of vinculin (*a, upper panel*). After treatment, adhesion plaques showed decreases in both darkness and size in IRM images (*arrows, lower panels*). Vinculin changed from elongated patches into small aggregates (*arrows, upper panels*). Bar, 10 μm.

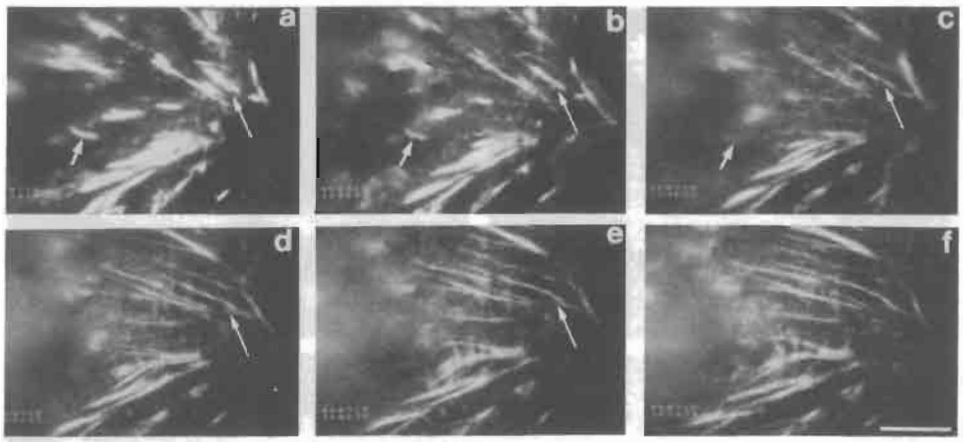

Fig. 6. High magnification micrographs of the dispersion of aggregates and the formation of stress fibers during recovery from ATP depletion. A mouse 3T3 cell, previously microinjected with IATR α-actinin, was treated with NaN_3 and 2-deoxyglucose for 2 h. The agents were then washed off at 15:33. Time of recording is indicated at lower left corner of each micrograph. Fluorescence images were recorded at 1 min (*a*), 5 min (*b*), 12 min (*c*), 22 min (*d*), 33 min (*e*), and 41 min (*f*) after removal of the agents. Some aggregates dispersed totally (*a–c, short arrows*); others showed an initial decrease in fluorescence, but later served as initiation sites for the assembly of stress fibers (*a–e, long arrows*). Bar, 10 μm.

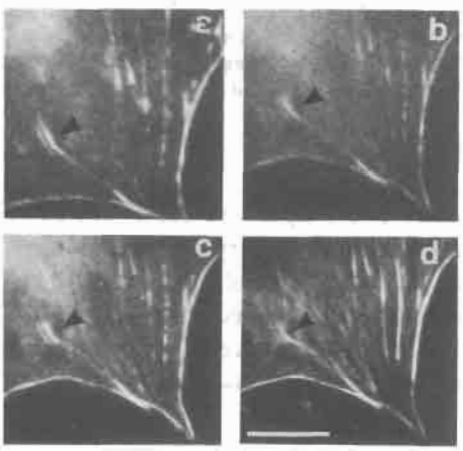

Fig. 7. Correlation between distribution of microinjected α-actinin and endogenous actin in a cell still recovering from ATP depletion. A mouse 3T3 cell, previously microinjected with IATR α-actinin, was treated with NaN_3 and 2-deoxyglucose for 2 h. The distribution of IATR α-actinin in living cells (*a*) before; (*b*) 6 min after removal of the agents was recorded. Most aggregates had undergone partial dispersion by this time. The cell was then fixed, stained with fluorescein–phalloidin, and observed with filter sets which select for either (*c*) rhodamine or (*d*) fluorescein. The distribution of α-actinin and actin at isolated aggregates was similar (*arrowheads*). However, some fibers showed continuous distribution of actin but punctate α-actinin. Bar, 20 μm.

Fig. 8. Reorganization of vinculin and formation of adhesion plaques during recovery from ATP depletion. A mouse 3T3 cell, previously microinjected with TRITC vinculin, was treated with NaN_3 and 2-deoxyglucose for 2 h. The agents were then washed off and fluorescence images (*upper panels*) and IRM images (*lower panels*) were recorded at approx. 9 min (*a*), 29 min (*b*), 59 min (*c*), and 120 min (*d*) after removal of agents. Vinculin aggregates underwent a gradual expansion into the elongated morphology typical of untreated cells (*arrows, upper panels*). Adhesion plaques also recovered concomitantly (*arrows, lower panels*). Bar, 10 μm.

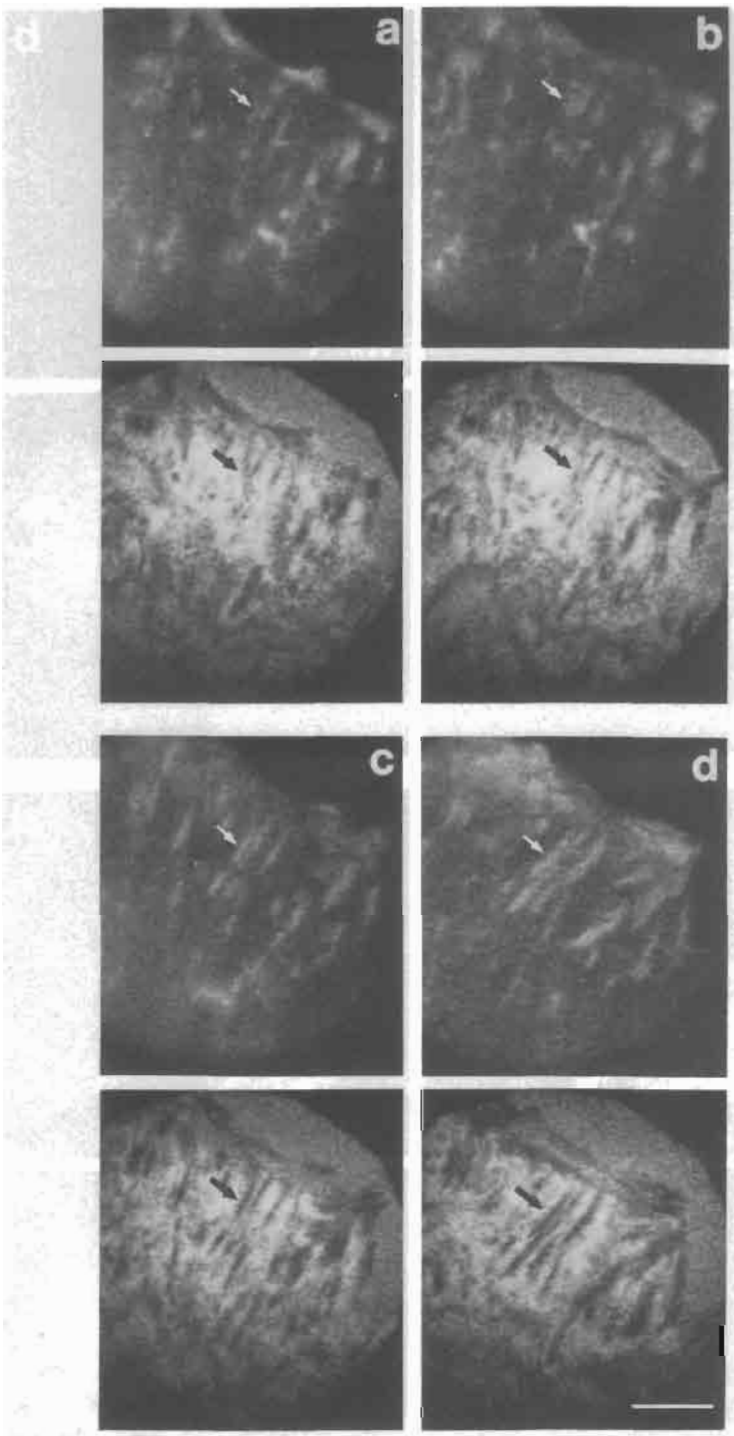

Fig. 8

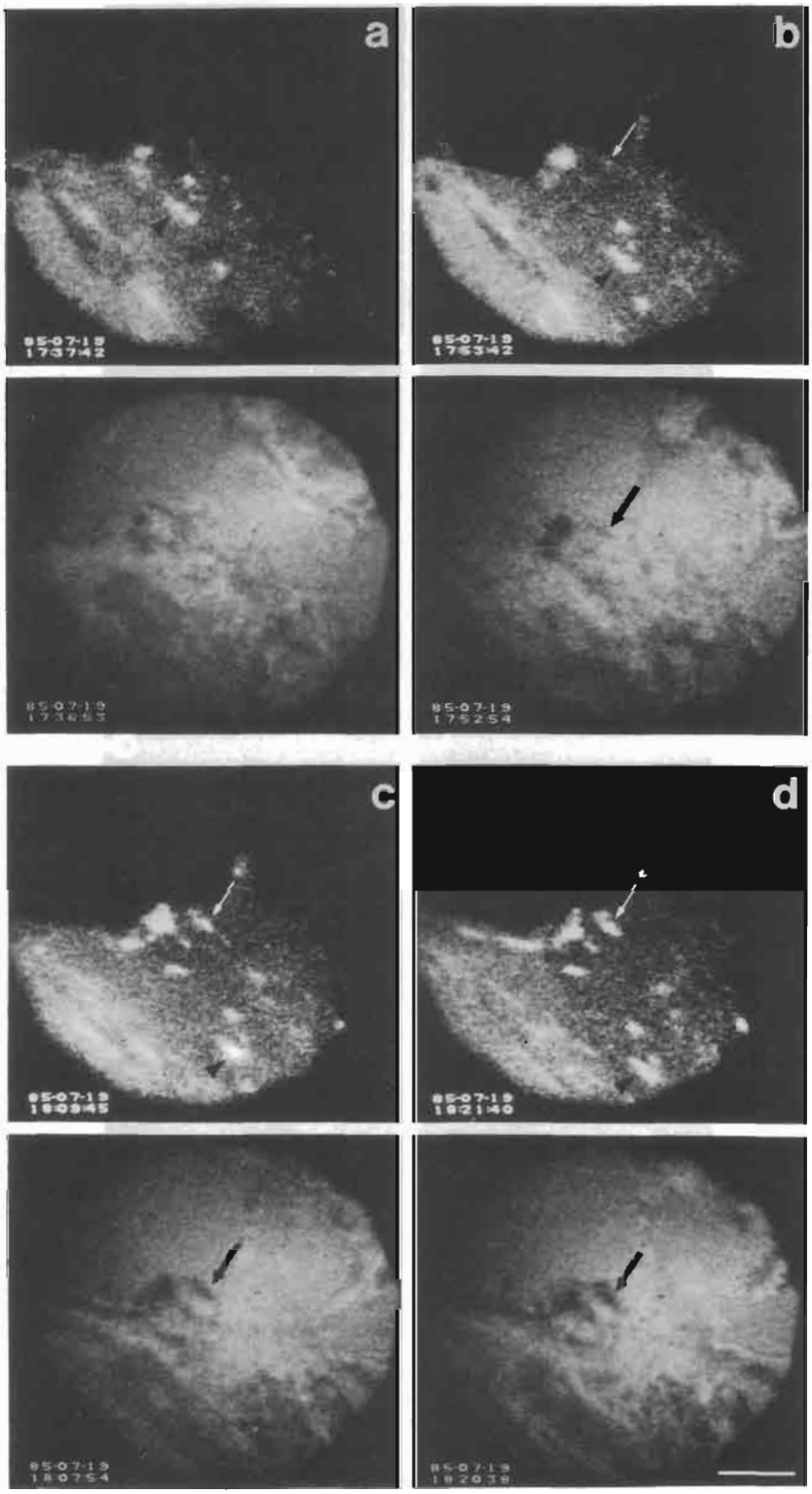
a
b
c
d
85-07-19
17:37:42
85-07-19
17:53:42
85-07-19
17:52:54
85-07-19
18:09:45
85-07-19
18:21:40
85-07-19
18:07:54
85-07-19
18:20:38

Fig. 9

IRM images indicated that focal contacts recovered gradually over a period of 2 h (figs 8, 9). The dark focal contacts in IRM images colocalized with vinculin aggregates which recovered into elongated plaques and with vinculin plaques which formed *de novo*, but not with those which moved into the perinuclear region (fig. 9).

In summary, although the net effects of ATP depletion on microfilaments have been demonstrated previously, the results here show clearly how the disrupted state can be reached through contraction of stress fibers and shrinkage of adhesion plaques, and how the normal morphology can be re-established during recovery through dispersion of aggregates, assembly of new stress fibers, and direct elongation of vinculin-containing aggregates. It is known that disruption of stress fibers, similar to that observed here, can be induced by various different agents, including trypsin [5] and 12-*O*-tetradecanoylphorbol-13-acetate (TPA, [11]). However, neither trypsin nor TPA induces contraction of stress fibers. In addition, after the addition of TPA, neither adhesion plaques nor vinculin plaques undergo rapid changes as observed here. Clearly, multiple pathways exist for the disruption of stress fibers. Our current effort is focused on viral transformation, which induces a similar disappearance of stress fibers and formation of vinculin- and α-actinin-containing aggregates [1, 6, 21]. It has been suggested that transformation may inhibit the maturation of the aggregates into adhesion plaques [21]. The present approach should yield important clues regarding the actual pathways involved in the disruptive process.

The author would like to thank Drs N. M. McKenna, C. S. Johnson and S. Stickel for reading the manuscript and C. S. Johnson and S. Stickel for technical assistance. This study was supported by grants from American Cancer Society (CD-200), Muscular Dystrophy Association, and National Science Foundation (PCM-8306971), and performed at the Doris W. Neustadt Laboratory of Cellular Structure at the National Jewish Center for Immunology and Respiratory Medicine.

REFERENCES

1. Maness, P F, Cell and muscle motility (ed R M Dowben & J W Shaw) vol. 1, p. 335. Plenum Press, New York (1981).
2. Geiger, B, Cell 18 (1979) 193.
3. Burridge, K & Feramisco, J R, Cell 19 (1980) 587.
4. Burridge, K & Connell, L, J cell biol 97 (1983) 359.
5. Badley, R A, Woods, A, Carruthers, L & Rees, D A, J cell sci 43 (1980) 379.

Fig. 9. Reorganization of vinculin and formation of adhesion plaques during recovery from ATP depletion. A mouse 3T3 cell, previously microinjected with TRITC vinculin, was treated with NaN_3 and 2-deoxyglucose for 2 h. The agents were then washed off at 17:35. Time of image recording is indicated at lower left corner of each micrograph. Fluorescence images (*upper panels*) and IRM images (*lower panels*) were recorded at approx. 2 min (*a*), 18 min (*b*), 33 min (*c*), and 46 min (*d*) after removing the agents. Some aggregates moved toward the nucleus and never developed into adhesion plaques (*arrowheads*). A group of three vinculin plaques formed *de novo* (*arrows*), with the concomitant appearance of dark patches in IRM images. Bar, 10 μm.

6. Vasiliev, J M, Biochim biophys acta 780 (1985) 21.
7. Bershadsky, A D, Gelfand, V I, Svitkina, T M & Tint, I S, Exp cell res 127 (1980) 421.
8. Sanger, J W, Sanger, J M & Jockusch, B M, Eur j cell biol 31 (1983) 197.
9. Taylor, D L & Wang, Y-L, Proc natl acad sci US 75 (1978) 857.
10. Wang, Y-L, Heiple, J M & Taylor, D L, Methods in cell biology (ed L Wilson) vol. 25, part b, p. 1. Academic Press, New York (1981).
11. Meigs, J B & Wang, Y-L, J cell biol 102 (1986) 1430.
12. Evans, R R, Robson, R M & Stromer, M H, J biol chem 259 (1984) 3916.
13. MacLean-Fletcher, S D & Pollard, T D, J cell biol 85 (1980) 414.
14. Wang, Y-L, J cell biol 99 (1984) 1478.
15. Amato, P A, Unanue, E R & Taylor, D L, J cell biol 96 (1983) 750.
16. Lazarides, E & Burridge, K, Cell 6 (1975) 289.
17. Feramisco, J R, Proc natl acad sci US 76 (1979) 3967.
18. Kreis, T E & Birchmeier, W, Cell 22 (1980) 555.
19. Avnur, Z & Geiger, B, J mol biol 153 (1981) 361.
20. Couchman, J R, Badley, R A & Rees, D A, J mus res cell motil 4 (1983) 647.
21. Bershadsky, A D, Tint, I S, Neyfakh Jr, A A & Vasiliev, J M, Exp cell res 158 (1985) 433.

Received November 19, 1985
Revised version received May 29, 1986

Printed in Sweden